MIT Libraries | DSpace@MIT

MIT Open Access Articles

Limits of power production due to finite membrane area in pressure retarded osmosis

The MIT Faculty has made this article openly available. ***Please share*** how this access benefits you. Your story matters.

Citation: Banchik, Leonardo H., Mostafa H. Sharqawy, and John H. Lienhard V. "Limits of power production due to finite membrane area in pressure retarded osmosis." Journal of Membrane Science 468 (15 October 2014), pp. 81–89.

As Published: http://dx.doi.org/10.1016/j.memsci.2014.05.021

Publisher: Elsevier

Persistent URL: http://hdl.handle.net/1721.1/103172

Version: Author's final manuscript: final author's manuscript post peer review, without publisher's formatting or copy editing

Terms of use: Creative Commons Attribution-Noncommercial-Share Alike

Massachusetts Institute of Technology

Limits of Power Production Due to Finite Membrane Area in Pressure Retarded Osmosis

Leonardo D. Banchik[1], Mostafa H. Sharqawy[2], John H. Lienhard V[*, 1]

[1] Department of Mechanical Engineering, Massachusetts Institute of Technology, Cambridge, MA 02139-4307, USA
[2] Department of Mechanical Engineering, King Fahd University of Petroleum and Minerals, Dhahran 31261, Saudi Arabia

Abstract

Dimensionless analytical expressions for the power attainable from an ideal counterflow pressure retarded osmosis (PRO) system model are developed using a one-dimensional model that accounts for streamwise variations in concentration. This ideal PRO system has no salt permeation or concentration polarization. The expressions show that the optimal hydraulic pressure difference, for which the maximum power is produced, deviates significantly from the classical solution of one-half of the trans-membrane osmotic pressure difference, $\Delta\pi/2$, as the dimensionless membrane area (MTU_π) increases and the ratio of draw to feed mass flow rates (MR) varies. The overall maximum power attainable from a PRO membrane is found to occur in the limit of infinitely large MTU_π (an effectiveness of unity) and infinite MR. For an ideal PRO system which mixes seawater (35 g/kg) and river water (1.5 g/kg), the overall maximum power of 1.57 kJ per kilogram of feed can be attained at roughly MTU_π of 15, an MR of 10, and a pressure of $0.83\Delta\pi$. Due to economic considerations, a PRO system in practice will have limited membrane area and will operate at an effectiveness of less than unity. The present work can be used to estimate the operating conditions and area required for a PRO system of given performance. The effect of concentration polarization on optimal hydraulic pressure difference and maximum power performance is also investigated using a numerical model.

Keywords

Pressure retarded osmosis, effectiveness-mass transfer units, heat and mass transfer analogy, concentration polarization

[*] Corresponding author
Email address: lienhard@mit.edu (John H. Lienhard V), Tel. +1 617-253-1000

Nomenclature

A	water permeability coefficient	kg m^{-2} s^{-1} kPa^{-1}
A_m	total membrane surface area	m^2
C	modified van 't Hoff coefficient	kPa kg g^{-1}
k_d	average draw side external mass transfer coefficient	m s^{-1}
K	average solute mass transfer resistance	s m^{-1}
$\dot{m}$	mass flow rate	kg s^{-1}
P	hydraulic pressure	kPa
P^*	pressure ratio	-
x	membrane position in the axial direction	m
w	salinity - grams of solutes per kg of solution	g kg^{-1}
$\dot{W}$	power	kW

Greek symbols

β	concentration polarization modulus	-
ε	effectiveness	-
η	combined turbine and generator efficiency	-
θ	osmotic pressure ratio	-
π	osmotic pressure	kPa
ρ	density	kg m^{-3}

Subscripts

d	draw
f	feed
in	inlet
o, out	outlet
p	permeate
P	based on a hydraulic pressure difference
π	based on an osmotic pressure difference
s	salt

Abbreviations

CP	concentration polarization
FO	forward osmosis
MR	mass flow rate ratio
MTU	mass transfer units
NTU	number of transfer units
PRO	pressure retarded osmosis
RR	recovery ratio

1. Introduction

Pressure retarded osmosis (PRO) is a variant of forward osmosis in which a pressurized concentrated draw stream and a more dilute feed stream are separated by a semi-permeable membrane, so that the permeate from the feed can enter the draw stream in a pressurized state from which useful power may be extracted.

We investigate the effect of streamwise length on the maximum power production and optimal trans-membrane pressure difference for a single, one-dimensional PRO mass exchanger model. A one-dimensional model takes into account changing concentrations and net driving pressures along the length of the membrane. This is unlike the classical "zero-dimensional" PRO model [1] which assumes that the net driving pressure is constant throughout the length of the exchanger. That approximation is valid for small, coupon-sized membranes in a benchtop experiment for which the stream compositions are constant along either side of the membrane; but for systems at the scale of a PRO power plant, the flow paths are much longer, so that the streamwise change in salinity, and consequently the change in flux, must usually be considered.

Studies of the power production possible with PRO systems have often been based on the zero-dimensional approximation model [1-10]. Under that model, the power produced by the system, comprised of an exchanger, a pump, and a turbine, is linearly proportional to the membrane area. Unlike the zero-dimensional case, a one-dimensional model shows that the power produced approaches a limiting value as the system area increases.

Papers which study one-dimensional PRO and forward osmosis (FO) exchanger models can be found in the literature [11-18], but these either consider only the performance in the limit of very large exchangers or only consider a small number of

specific operating conditions. For example, Feinberg *et al.* [11] considered a PRO osmotic energy recovery device which operates at the point where the hydraulic pressure and the osmotic pressure differences are equal. While this can yield an overall maximum power, a very large membrane area will be required and a system with a smaller area is likely to be used in practice. The overall maximum power is attainable with an infinitely large exchanger (effectiveness of unity), a large mass flow rate ratio, and the optimum balance of hydraulic to osmotic pressures.

Kim *et al.* [12] and van der Zwan *et al.* [13] numerically integrated the permeate flux, feed concentration, and draw concentration for a one-dimensional PRO system model of a single finite size. In the forward osmosis literature, Xiao *et al.* [14] developed a one-dimensional mathematical model with dimensionless variables for parallel-flow and counterflow hollow fiber FO exchangers. Computational fluid dynamics simulations were also performed for one- and two-dimensional FO exchangers of a single finite size [15-17].

By thermodynamic analysis, without consideration of transport processes, Yip *et al.* [18] found expressions for the optimal pressure difference and overall maximum power in a PRO system. The results coincide with the results of the present model for a perfectly effective, i.e., very large, PRO exchanger because the overall maximum power is limited by thermodynamic considerations and not by the membrane properties or configuration. The membrane properties and configuration, however, will dictate the size of the exchanger required to produce a given amount of power. The present work describes system behavior between the zero-dimensional (very small) and perfectly effective (very large) PRO exchanger by accounting for transport processes along the membrane, and it

can therefore be used to estimate the area of a PRO exchanger required to produce a given amount of power.

In the present study, we find expressions for the limiting maximum power attainable for given draw and feed stream salinities. The expressions are dimensionless and allow for a wide range of exchanger sizes, membrane permeability coefficients, mass flow rates, and hydraulic pressure differences to be considered. The expressions are valid for an ideal system, i.e., a membrane system without salt permeation and concentration polarization. It is found that the hydraulic pressure difference which provides the maximum power deviates significantly from the classical optimum of one-half of the trans-membrane osmotic pressure, $\Delta\pi/2$, as the dimensionless area of the exchanger increases and as the ratio of mass flow rates into the exchanger changes. As the exchanger becomes very large (i.e., approaches an effectiveness of unity), the maximum amount of permeate will be attained and the overall maximum power can be produced. We find expressions for the overall maximum power and for the optimal hydraulic pressure which corresponds to this point. Due to economic considerations that can limit membrane area, a PRO system in practice will operate at an effectiveness of less than unity. The results of the present analysis can be used to estimate the operating conditions and area required for a PRO system of finite size.

The present paper modifies an analytical solution for flux in a one-dimensional, ideal PRO mass exchanger by Sharqawy *et al.* [19]. The modification allows for the inclusion of an important dimensionless quantity, the pressure ratio, which is necessary for power performance analysis. Because the analytical solution does not consider the effect of concentration polarization or salt permeation within the exchanger, and because these

phenomena effectively increase the resistance to mass transfer within the exchangers, the power performance results from the analytical expressions are upper bounds on performance. The impact of concentration polarization on the maximum power is investigated numerically later in the paper.

For more detail on PRO membrane chemistry and fouling the reader is directed to [20].

2. Modified PRO Mass Exchanger Flux Performance Model

In the derivations that follow, only a counterflow PRO exchanger is considered because osmotic mass exchangers, like heat exchangers, operate most effectively when the driving force is uniformly maintained throughout the length of the exchanger as is the case in the counterflow orientation [19].

The PRO water transport equation for a differential area of membrane, based on the solution-diffusion model [1], is given by

$$d\dot{m}_p(x) = A(\Delta\pi(x) - \Delta P)dA_m(x) \tag{1}$$

where: $d\dot{m}_p(x)$ [kg/s] is the differential mass flow rate of pure water which permeates through the membrane from the feed to the draw side as a function of axial distance along the exchanger; A [kg/s-m^2-kPa] is the mass-based water permeability coefficient; $\Delta\pi(x)$ [kPa] is the trans-membrane osmotic pressure difference which is allowed to vary axially throughout the membrane (i.e. $\pi_{draw}(x) - \pi_{feed}(x)$); ΔP [kPa] is the trans-membrane hydraulic pressure difference (i.e. $P_{draw} - P_{feed}$); and $dA_m(x)$ [m^2] is the differential membrane area.

In the following derivation, it is assumed that the water permeability coefficient is constant, concentration polarization effects are neglected, there is no salt permeation, the hydraulic pressure drop through both flow channels is negligible, and the osmotic pressure is a linear function of salinity according to van ’t Hoff’s law. The effect of concentration polarization on optimal operating conditions and power performance will be investigated in a later section.

By combining the differential PRO water transport equation and conservation of mass for solutes and solutions around the feed and draw stream as control volumes, Eq. (2) can be obtained (see [19] for detail):

$$d\dot{m}_p(x) = A\left[\frac{\dot{m}_{d,out}\pi_{d,out}}{\dot{m}_{d,out}-\dot{m}_p(x)} - \frac{\dot{m}_{f,in}\pi_{f,in}}{\dot{m}_{f,in}-\dot{m}_p(x)} - \Delta P\right] dA_m(x) \tag{2}$$

Eq. (2) is now cast in a dimensionless form. Five dimensionless parameters are introduced for this purpose.

Recovery ratio, *RR*

$$RR \equiv \frac{\dot{m}_p}{\dot{m}_{f,in}} \tag{3}$$

The recovery ratio is the total mass flow rate of permeate recovered from the feed stream divided by the mass flow rate of the incoming feed stream. The recovery ratio should not be confused with the effectiveness which will be described later.

Mass flow rate ratio, *MR*

$$MR \equiv \frac{\dot{m}_{d,in}}{\dot{m}_{f,in}} \tag{4}$$

The mass flow rate, or mixing, ratio is the mass flow rate of the draw solution divided by that of the feed solution at the inlet of the PRO mass exchanger.

Osmotic pressure ratio, θ

For the draw side: $\theta_d \equiv \frac{\pi_{d,in}}{\Delta\pi_{max}}$ (5)

For the feed side: $\theta_f \equiv \frac{\pi_{f,in}}{\Delta\pi_{max}} = \theta_d - 1$ (6)

where $\Delta\pi_{max} \equiv \pi_{d,in} - \pi_{f,in}$ (7)

The osmotic pressure ratio is the ratio of the osmotic pressure at the draw or feed inlet to the maximum osmotic pressure difference. The maximum osmotic pressure difference is simply equal to the difference in the inlet osmotic pressures of the draw and feed. For PRO exchanger operation, θ_d will always be greater than θ_f.

Pressure ratio, P^*

$$P^* \equiv \frac{\Delta P}{\Delta\pi_{max}} \quad (9)$$

The pressure ratio is the hydraulic pressure difference divided by the maximum osmotic pressure difference. When $P^* = 1$, the trans-membrane hydraulic pressure difference is equal to the maximum osmotic pressure difference and there is no flux through the exchanger, per Eq. (1). At the other limit, when $P^* = 0$, the exchanger operates in the direct forward osmosis (FO) regime and the maximum amount of flux permeates through the membrane.

Mass Transfer Units, MTU_π

$$MTU_{\pi} \equiv \frac{A_m A \Delta\pi_{max}}{\dot{m}_{f,in}} \tag{8}$$

The number of *mass transfer units* (MTU) is a dimensionless parameter for a membrane mass exchanger similar to the *number of transfer unit*s (NTU) used in heat exchanger rating and sizing [22, 23]. The total membrane area, A_m, is similar to the total heat exchanger surface area and A is the overall water permeability coefficient which is analogous to the overall heat transfer coefficient in heat exchangers. The number of mass transfer units based on the hydraulic pressure difference, which is used in the solution in [19], could be denoted as MTU_P and is related to MTU_π by the equality $MTU_P = MTU_\pi \times P^*$ in which P^* is the pressure ratio.

For the counterflow model, we may more conveniently define two additional dimensionless variables from the earlier variables so that we may express the recovery ratio as a function of the inlet flow conditions. Equations (10) and (11) can be derived by applying conservation of mass to the whole exchanger.

Outlet mass flow rate ratio, MR_o

$$MR_o \equiv \frac{\dot{m}_{d,out}}{\dot{m}_{f,in}} = MR + RR \tag{10}$$

Osmotic pressure ratio at draw outlet, $\theta_{d,o}$

$$\theta_{d,o} \equiv \frac{\pi_{d,out}}{\Delta\pi_{max}} = \theta_d \frac{MR}{MR+RR} \tag{11}$$

Using these dimensionless groups, Eq. (2) can be rewritten in a dimensionless form as follows:

$$dRR(x) = \left(\frac{MR_o \theta_{d,o}}{MR_o - RR(x)} - \frac{\theta_f}{1-RR(x)} - P^*\right) dMTU_{\pi}(x) \tag{12}$$

Equation (12) can be integrated as in Eq. (13) where the interval on the left hand side integral is from zero to the total recovery ratio:

$$\int_0^{RR}\left(\frac{MR_o\theta_{d,o}}{MR_o-RR(x)}-\frac{\theta_f}{1-RR(x)}-P^*\right)^{-1}dRR(x)=MTU_\pi \tag{13}$$

which may be simplified to

$$\int_0^{RR}\frac{(MR_o-RR(x))(1-RR(x))}{(RR(x)-\kappa)(RR(x)-\lambda)}dRR(x)=P^*MTU_\pi \tag{14}$$

where

$$\kappa=\frac{1}{2P^*}\left[\left(P^*+MR_o\left(P^*-\theta_{d,o}\right)+\theta_f\right)-\sqrt{\left(P^*+MR_o\left(P^*-\theta_{d,o}\right)+\theta_f\right)^2+4P^*MR_o\left(\theta_{d,o}-P^*-\theta_f\right)}\right] \tag{15}$$

$$\lambda=\frac{1}{2P^*}\left[\left(P^*+MR_o\left(P^*-\theta_{d,o}\right)+\theta_f\right)+\sqrt{\left(P^*+MR_o\left(P^*-\theta_{d,o}\right)+\theta_f\right)^2+4P^*MR_o\left(\theta_{d,o}-P^*-\theta_f\right)}\right] \tag{16}$$

The integration of Eq. (14) yields

$$MTU_\pi=\frac{(\lambda-1)(\lambda-MR_o)}{P^*(\kappa-\lambda)}\ln\left(\frac{\lambda-RR}{\lambda}\right)-\frac{(\kappa-1)(\kappa-MR_o)}{P^*(\kappa-\lambda)}\ln\left(\frac{\kappa-RR}{\kappa}\right)-\frac{RR}{P^*} \tag{17}$$

Therefore, Eq. (17) combined with Eqs. (10) and (11) can be used in the design of a membrane mass exchanger in which the required mass transfer units, effectively the membrane area, is given as an explicit relation of the form

$$MTU_\pi=f(RR,MR,\theta_d,P^*) \tag{18}$$

3. PRO Counterflow Mass Exchanger Effectiveness

The effectiveness is the recovery ratio divided by the maximum recovery ratio, which is determined by the thermodynamic permeation limit of the exchanger as given by Eq. (19):

$$\varepsilon\equiv\frac{RR}{RR_{max}} \tag{19}$$

Using Eq. (1), the maximum permeate in the case of counterflow configuration will occur when the hydraulic pressure difference is equal to the osmotic pressure difference at one side of the exchanger. Therefore, there are two conditions at which the driving force for permeate flow will become zero. The first is at the side of the exchanger where the feed enters and the draw exits:

$$\pi_{d,out} - \pi_{f,in} = \Delta P \tag{20}$$

Using the van 't Hoff model of linearly proportional osmotic pressure to salinity, and applying conservation of solution and solute, this condition will lead to

$$RR_{max,1} = MR\left(\frac{\theta_d}{P^* + \theta_f} - 1\right) \tag{21}$$

The second condition occurs at the side of the exchanger where the draw enters and the feed stream exits:

$$\pi_{d,in} - \pi_{f,out} = \Delta P \tag{22}$$

and

$$RR_{max,2} = 1 - \frac{\theta_f}{\theta_d - P^*} \tag{23}$$

Since there are two limits for the maximum recovery ratio, we should take the minimum value, hence:

$$RR_{max} = \min\langle RR_{\max,1},\ RR_{\max,2}\rangle \tag{24}$$

The effectiveness is defined by Eq. (19) and the recovery ratio can be written in terms of the effectiveness and maximum recovery ratio. Substituting Eq. (19) into Eq. (17), an expression for MTU_π as a function of the effectiveness can be obtained as given in Eq. (25):

$$MTU_\pi = \frac{(\lambda-1)(\lambda-MR_o)}{P^*(\kappa-\lambda)}\ln\left(\frac{\lambda-\varepsilon RR_{max}}{\lambda}\right) - \frac{(\kappa-1)(\kappa-MR_o)}{P^*(\kappa-\lambda)}\ln\left(\frac{\kappa-\varepsilon RR_{max}}{\kappa}\right) - \frac{\varepsilon RR_{max}}{P^*} \tag{25}$$

There are two problems of interest for which the derived expressions can be used: sizing and rating PRO mass exchangers. For sizing, the desired recovery ratio, effectiveness, or power production (as seen in the following section) is supplied along with MR, θ_d, θ_f, and P* to estimate the exchanger's MTU_π. For rating, the effectiveness of an existing exchanger can be determined from the exchanger's MTU_π, MR, θ_d, θ_f, and P*. From this analysis, a designer can estimate how well an exchanger is performing relative to how well it can perform.

4. PRO Power Production

Figure 1 shows a simplified PRO system that takes in a draw and feed stream. The PRO system shown is simplified because it does not contain several components necessary for operation: a pressure exchanger, a feed-side pump, or pre-treatment for either working fluid. The draw stream is brought into the system and pumped to a hydraulic pressure which corresponds with optimum power performance. The feed and pressurized draw streams enter a PRO mass exchanger in counterflow where an amount of permeate is forced through a semi-permeable membrane into the draw stream. The diluted draw stream which exits the exchanger is depressurized through a hydro-turbine and it is assumed that a portion of the draw stream equal to the mass flow rate of the total permeate provides the net power output while the remaining draw solution provides the power required to run the pump. This assumption implies that the depressurization of the remaining draw solution and the pressurization of the incoming draw stream are done in an isentropic manner.

We can determine the amount of useful power achievable from the permeate depressurization by calculating the power produced from a change in hydraulic pressure for an incompressible fluid

$$\dot{W} = \eta \frac{\dot{m}_p}{\rho_{d,o}} \Delta P \tag{26}$$

where the density ρ is equal to the density of the diluted outlet draw stream, ΔP is the pressure drop across the hydro-turbine, and η is the combined turbine and generator efficiency. Because we have assumed no pressure drops in the exchanger and we consider that the feed stream is at atmospheric pressure within the exchanger, ΔP is equal to the PRO trans-membrane hydraulic pressure.

4.1 Zero-Dimensional Model for a Very Small Exchanger

For a zero-dimensional model, the osmotic pressure and permeate do not vary within the exchanger. Therefore, substituting the integral form of Eq. (1) into Eq. (26) and differentiating with respect to ΔP, it can be shown that the maximum power occurs when $\Delta P = \Delta\pi/2$. This result was first shown by Lee *et al.* [1] and corresponds to an optimal pressure ratio of $P^*_{opt} \equiv \frac{\Delta P}{\Delta \pi} = 1/2$. Therefore, for an exchanger small enough that a zero-dimensional model applies, $\Delta\pi = \Delta\pi_{max}$, and it can be shown that the maximum power per unit mass flow rate of the feed stream is linearly proportional to MTU_π and $\Delta\pi_{max}$ Eq. (27):

$$\frac{\dot{W}_{max,0-D}}{\dot{m}_{f,in}} = \frac{\eta}{\dot{m}_{f,in}} \frac{A_m A}{\rho_{d,o}} \frac{\Delta\pi^2}{4} = \frac{\eta MTU_\pi}{\rho_{d,o}} \frac{\Delta\pi_{max}}{4} \tag{27}$$

4.2 One-Dimensional Model for a Finite Size Exchanger

To find the power producible by a finite-size exchanger, we use the analytical expressions of the one dimensional model derived earlier to determine the permeation flow rate through the membranes. Dividing Eq. (26) by $\dot{m}_{feed,in}$ and substituting the relevant dimensionless parameters yields the following expression for the specific power of a finite-size exchanger relative to an inlet feed stream of one kilogram per second, Eq. (28):

$$\frac{\dot{W}_{1-D}}{\dot{m}_{f,in}} = \frac{\eta\,\Delta\pi_{max}}{\rho_{d,o}} RR \cdot P^{*} \tag{28}$$

Using Eqs. (15)-(17) and (28), the specific power output can be plotted versus the full range of the pressure ratio for a given value of MTU_{π} and contours of MR as shown in Fig. 2. The inlet salinities considered in this analysis are $w_{d,in}$ = 35 g/kg and $w_{f,in}$ = 1.5 g/kg, which are representative of seawater and river water, respectively. The modified van 't Hoff coefficient which corresponds to these salinities, assuming the solute weight fractions are proportional to those found in seawater, is $C = 73.07$ kPa-kg/g (see [19, 21] for details). The combined turbine and generator efficiency is assumed to be unity in order to determine the maximum power. It can be seen that a maximum power occurs at a unique intermediate value of the pressure ratio for a given mass flow rate ratio.

The pressure ratio P^{*}_{opt} at which the maximum power occurs is found by using the Golden Section search numerical optimization method in EES [24]. By substituting the numerical value of this optimal pressure ratio into Eq. (28), the maximum specific power $\dot{W}_{max}/\dot{m}_{f,in}$ can be determined. Figures 3 and 4 show the specific maximum power and the optimal pressure ratio versus MTU_{π} for contours of the mass flow rate ratio. Figure 3 shows that the specific maximum power increases for increasing MTU_{π} and increasing

MR. At roughly MTU_π = 10 and MR = 4, the overall maximum specific power is nearly reached at an optimal pressure ratio of roughly 0.73.

Figure 3 also shows the maximum specific work predicted by the zero-dimensional model, which is determined by drawing the tangent of the slope of the specific power vs. MTU_π where MTU_π approaches zero. The tangent can be drawn because the specific power for the zero-dimensional model is linearly proportional to MTU_π. From this, it is apparent that using the zero-dimensional approximation for prediction of power production in a large exchanger can result in a severe underestimation of required area. Referring to Fig. 3, for a given maximum specific power production of 1.5 kJ/kg at MR=10, the zero-dimensional model predicts MTU_π = 2.5 and the one-dimensional model predicts MTU_π = 6. This corresponds to increasing MTU_π, and consequently membrane area, by a factor of 2.4.

To produce the overall maximum specific power (where MTU_π and MR approach infinity) with an ideal PRO would require very large membrane area and an effectiveness approaching unity. Due to economic considerations, a PRO system in practice will have some limited area and a lower effectiveness. From Eq. (25), at an effectiveness of 0.95 and a draw to feed mass flow rate ratio of 4, the amount of power producible with an ideal PRO exchanger will be 1.23 kJ per kilogram of feed at an optimal pressure of $0.6\Delta\pi$ and an MTU_π of 3.49.

4.2.1 Overall Maximum Power and Optimal Pressure Ratio

The overall maximum power achievable for a combination of any two inlet salinities is found when MR and MTU_π approach infinity, the latter of which corresponds to an

exchanger effectiveness of unity. The overall maximum specific power can be found by substituting Eqs. (19) and (24) into Eq. (28) and taking effectiveness as unity:

$$\frac{\dot{W}_{1-D}}{\dot{m}_{f,in}} = \frac{\eta\,\Delta\pi_{max}}{\rho_d} \min\left\langle MR\left(\frac{\theta_d}{P^*+\theta_f} - 1\right),\ 1 - \frac{\theta_f}{\theta_d - P^*}\right\rangle \cdot P^* \tag{29}$$

We only take the second term in the minimum operator when MR goes to infinity which yields:

$$\frac{\dot{W}_{1-D}}{\dot{m}_{f,in}} = \frac{\eta\,\Delta\pi_{max}}{\rho_{d,o}}\left(1 - \frac{\theta_f}{\theta_d - P^*}\right) P^* \tag{30}$$

To find the overall maximum of the specific power, we take the first derivative of Eq. (30) with respect to P^* and equate it to zero:

$$\frac{\partial}{\partial P^*}\left(\frac{\dot{W}_{1-D}}{\dot{m}_{f,in}}\right) = \frac{\partial}{\partial P^*}\left[\frac{\eta\,\Delta\pi_{max}}{\rho_{d,out}}\left(1 - \frac{\theta_f}{\theta_d - P^*}\right) P^*\right] = 0 \tag{31}$$

This results in a simple quadratic equation which we use to determine the optimal pressure ratio P^*_{opt}:

$$P^*_{opt} = \theta_d \pm \sqrt{\theta_d \theta_f} \tag{32}$$

We verify Eq. (32) by using it to predict the optimal pressure ratio for a seawater and river water combination. Using Eq. (32), P^*_{opt} = 0.83 which is the same as the value in Fig. 4 to which the MR = 10 contour asymptotes for large MTU_π.

The negative root in Eq. (32) is taken to ensure that P^*_{opt} is a number between the bounds of P^* (zero and unity). Substituting that root from Eq. (32) into Eq. (30), we determine the overall maximum specific power as a function of the inlet salinities, the density of the outlet draw solution, and a modified van ‘t Hoff coefficient:

$$\frac{\dot{W}_{global\,max,1-D}}{\dot{m}_{f,in}} = \frac{\eta\,\Delta\pi_{max}}{\rho_d}\left(\theta_d - 2\sqrt{\theta_d \theta_f} + \theta_f\right) \tag{33}$$

For seawater and river water, $w_{d,in}$ = 35 g/kg and $w_{f,in}$ = 1.5 g/kg, we find the overall maximum specific power to be 1.57 kJ per kilogram of river water using Eqs. (32) and (33). Results for other stream combinations as well as the modified van 't Hoff coefficients used are displayed in Table 1.

The values of specific work displayed in Table 1 are upper bounds and will decrease with the addition of loss mechanisms to the transport model. For inefficiencies in the turbine, the results can be de-rated via multiplication by an efficiency factor of less than unity. Power consumption by any pumps can be considered by subtracting the power required for pumping from the de-rated turbine power.

The inclusion of concentration polarization, salt permeation, and hydraulic pressure losses will further decrease the power that can be produced in actuality. In the next subsection, we apply a numerical model that includes internal and external concentration polarization to determine the effect of these non-idealities on power production and optimal pressure.

4.2.2 Effect of Concentration Polarization on Optimal Pressure and Power Performance

A finite-difference model is numerically solved to determine the effect of internal and external concentration polarization on the maximum power and optimal pressure results. The integral form of the differential transport equation, Eq. (1), is modified to include two exponential concentration polarization (CP) moduli, as shown in Eq. (34), which relate the osmotic pressure in the bulk to the osmotic pressure at the membrane surface. The moduli come from applying conservation of salt to a control volume between the

bulk draw solution and the membrane (external CP) and between the membrane-support layer interface and bulk feed solution (for internal CP). These moduli are implicit functions of the permeate mass flow rate through each element and an average mass transfer coefficient k_d [m/s] for the draw side (external dilutive CP) and an average mass transfer resistance K [s/m] for the feed side (internal concentrative CP in the membrane support layer):

$$\dot{m}_p = A\left[\pi_{d,in}\exp\left(-\frac{\dot{m}_p}{k_d \cdot \rho_p \cdot A_m}\right) - \pi_{f,in}\exp\left(\frac{\dot{m}_p K}{\rho_p \cdot A_m}\right) - \Delta P\right] A_m \tag{34}$$

More details on the concentration polarization model used can be found in [25]. Equation (34) assumes an asymmetric membrane with the active layer facing the draw stream and no concentrative external CP on the feed side, which is acceptable for relatively dilute feed streams.

Equation (34), combined with conservation of solute and solvent, is applied to a series of discretized elements and numerically integrated in the streamwise direction. The equations were solved in Engineering Equation Solver [24] and the number of elements was increased to 200 by which point the results were seen to be grid independent. The model assumes that the osmotic pressure is linearly proportional to salinity, no salt permeation occurs, pure water permeates through the membrane, and there are no pressure losses through the exchanger. Model inputs and ranges are given in Table 2.

The total mass flow rate of permeate is found by numerically integrating the permeate flow rates of each element along the exchanger. The CP exponential moduli are numerically averaged across the exchanger to give β_d and β_f as given in Eqs. (35) and (36):

$$\beta_d = \frac{1}{A_m}\int_0^{A_m} \exp\left(-\frac{\dot{m}_p}{k_d \cdot \rho_p \cdot A_m}\right) dA_m \tag{35}$$

$$\beta_f = \frac{1}{A_m}\int_0^{A_m} \exp\left(\frac{\dot{m}_p\, K}{\rho_p \cdot A_m}\right) dA_m \tag{36}$$

Figures 5 and 6 show the specific maximum power and optimal pressure ratio vs. MTU_π with MR contours using the analytical model and the numerical model which considers concentration polarization. Both plots consider the case of mixing of seawater and river water. At very high MTU_π values, the numerical model nearly converges to the analytical one. Until that point, however, an exchanger with concentration polarization will require much more membrane area to produce a given amount of specific power. For instance, in order to produce 1.5 kJ/kg of power with MR = 10, an exchanger without CP will require MTU_π = 5.9. An exchanger with CP, however, will require MTU_π = 9.4, which corresponds to an increase in area by a factor of 1.6. For the membrane permeability coefficient given in Table 2, unity feed mass flow rate in kg/s, and $\Delta\pi_{max}$ = 2448 kPa for seawater and river water, area increases from 788 m^2 to 1255 m^2. Figure 6 shows that for MR > 1 over the range of MTU_π, CP effects decrease the optimal pressure ratio below that of the analytical model. For MR < 1, the effect is opposite and CP effects increase the optimal pressure ratio.

Figure 7 shows that the average CP moduli (β_d and β_f) in the exchanger decrease and approach unity as MTU_π increases for a range of MR in the case of combining seawater and river water. For the case of seawater and river water, the feed-side internal CP is a larger issue than the draw CP, a result in agreement with literature [2, 4, 25, 27]. Figure 7 also shows that the largest deviation of β from unity is for high values of MR at low

MTU_π, an effect which will limit the ideal mass flow rate ratio of infinity for overall maximum power.

Figure 8 shows the specific maximum power vs. MTU_π with MR contours using the analytical and numerical models for mixing: (a) brine and seawater ($w_{d,in}$ = 70 g/kg and $w_{f,in}$ = 35 g/kg, respectively); and (b) brine and wastewater or river water ($w_{d,in}$ = 70 g/kg and $w_{f,in}$ = 1.5 g/kg, respectively). Comparing Figs. 8a and 8b, the brine and seawater combination offers significantly lower power production than the brine and wastewater case regardless of concentration polarization effects. This poor performance is further exacerbated by an additional feed-side external concentration polarization term which should be considered when seawater is used as a feed. The additional feed-side external CP term was not considered in this analysis.

Figure 9 shows the optimal pressure ratio vs. MTU_π with MR contours using the analytical and numerical models for mixing (a) brine and seawater and (b) brine and wastewater or river water. In Fig. 9b, the numerical optimal pressure ratio for small MTU_π does not begin at 0.5 because of the severe external and internal concentration polarization resulting from these high salinities.

6. Conclusions

Dimensionless analytical expressions are developed for the power achievable in an ideal, counterflow PRO system using a one-dimensional model that accounts for streamwise changes in salinity. This ideal PRO system has no salt permeation or concentration polarization. From the one-dimensional PRO mass exchanger model, the zero-dimensional theoretical result that maximum power occurs at a hydraulic pressure

difference of one-half of the trans-membrane osmotic pressure difference is shown to be an idealization valid only for membranes with a very small dimensionless size, MTU_π. Significant deviations from this classical solution occur as MTU_π increases and as the ratio of draw to feed mass flow rate, MR, varies.

In the limit as both MTU_π approaches infinity (very large membrane area and an effectiveness approaching unity) and MR approaches infinity, an expression for the overall maximum power produced per unit of feed mass flow rate is found. This expression is in agreement with thermodynamic limits previously found in the literature. For an ideal PRO system which blends seawater (35 g/kg) and river water (1.5 g/kg), the overall maximum power of 1.57 kJ per kilogram of feed can be attained at MTU_π of 15, MR of 10, and a pressure of $0.83\Delta\pi$. In practice, PRO systems will generally operate at an effectiveness of less than unity. The results of the present analysis can be used to estimate the operating conditions and areas required for a PRO system of a given performance.

The presence of draw-side external and internal concentration polarization is numerically investigated and found to affect the optimal hydraulic pressures. Additionally, CP effects usually require more membrane area to be used to produce a given power than the ideal case.

Acknowledgements

The authors would like to thank King Fahd University of Petroleum and Minerals in Dhahran, Saudi Arabia, for funding the research reported in this paper through the Center for Clean Water and Clean Energy at MIT and KFUPM. This material is based upon

work supported by the National Science Foundation Graduate Research Fellowship Program under Grant No. 1122374.

References

[1] K. Lee, R. Baker, H. Lonsdale, Membranes for power generation by pressure-retarded osmosis, Journal of Membrane Science 8 (1981) 141–171.

[2] A. Achilli, T. Y. Cath, A. E. Childress, Power generation with pressure retarded osmosis: An experimental and theoretical investigation, Journal of Membrane Science 343 (2009) 42–52.

[3] G.Z. Ramon, B.J. Feinberg, E.M.V. Hoek, Membrane-based production of salinity-gradient power, Energy and Environmental Science, 4 (2011) 4423-4434.

[4] M.C.Y. Wong, K. Martinez, G.Z. Ramon, E.M.V. Hoek, Impacts of operating conditions and solution chemistry on osmotic membrane structure and performance, Desalination, 287 (2012) 340-349.

[5] J.W. Post, J. Veerman, H.V.M. Hamelers, G.J.W. Euverink, S.J. Metz, K. Nymeijer, C.J.N. Buisman, Salinity-gradient power: Evaluation of pressure-retarded osmosis and reverse electrodialysis, Journal of Membrane Science, 288 (2007) 218-230.

[6] S. Chou, R. Wang, L. Shi, Q. She, C. Tang, A.G. Fane, Thin-film composite hollow fiber membranes for pressure retarded osmosis (PRO) process with high power density, Journal of Membrane Science, 389 (2012) 25-33.

[7] T. Thorsen, T. Holt, The potential for power production from salinity gradients by pressure retarded osmosis, Journal of Membrane Science, 335 (2009) 103-110.

[8] H. Enomoto, M. Fujitsuka, T. Hasegawa, M. Kuwada, A. Tanioka, M. Minagawa, A feasibility study of pressure-retarded osmosis power generation system based on measuring permeation volume using reverse osmosis membrane, Electrical Engineering in Japan, 173 (2010) 1129-1138.

[9] M.H. Sharqawy, S.M. Zubair, J.H. Lienhard V, Second law analysis of reverse osmosis desalination plants: an alternative design using pressure retarded osmosis, Energy, 36 (2011) 6617-6626.

[10] M.H. Sharqawy, S.M. Zubair, J.H. Lienhard V, Rebuttal to "Discussion of 'Second law analysis of reverse osmosis desalination plants: an alternative design using pressure retarded osmosis' [Energy 2011] 36: 6617-6626]", Energy, 46, 691-693..

[11] B.J. Feinberg, G.Z. Ramon, E.M.V. Hoek, Thermodynamic analysis of osmotic energy recovery at a reverse osmosis desalination plant, Environmental Science and Technology, 47 (2013) 2982-2989.

[12] J. Kim, M. Park, S.A. Snyder, J.H. Kim, Reverse osmosis (RO) and pressure retarded osmosis (PRO) hybrid processes: Model-based scenario study, Desalination, 322 (2013) 121-130.

[13] S. van der Zwan, I.W.M. Pothof, B. Blankert, J.I. Bara, Feasibility of osmotic power from a hydrodynamic analysis at module and plant scale, Journal of Membrane Science, 389 (2012) 324-333.

[14] D. Xiao, W. Li, S. Chou, R. Wang, C.Y. Tang, A modeling investigation on optimizing the design of forward osmosis hollow fiber modules, Journal of Membrane Science, 392-393 (2012) 76-87.

[15] M.F. Gruber, C.J. Johnson, C.Y. Tang, M.H. Jensen, L. Yde, C. Hélix-Nielsen, Computational fluid dynamics simulations of flow and concentration polarization in forward osmosis membrane systems, Journal of Membrane Science, 379 (2011) 488-495.

[16] D.H. Jung, J. Lee, D.Y. Kim, Y.G. Lee, M. Park, S. Lee, D.R. Yang, J.H. Kim, Simulation of forward osmosis membrane process: Effect of membrane orientation and flow direction of feed and draw solutions, Desalination, 277 (2011) 83-91.
[17] A. Sagiv, R. Semiat, Finite element analysis of forward osmosis process using NaCl solutions, Journal of Membrane Science, 379 (2011) 86-96.
[18] N.Y. Yip, M. Elimelech, Thermodynamic and energy efficiency analysis of power generation from natural salinity gradients by pressure retarded osmosis, Environmental Science and Technology, 46 (2012) 5230-5239.
[19] M.H. Sharqawy, L.D. Banchik, J.H. Lienhard V, Effectiveness-mass transfer units (ε-MTU) model of an ideal pressure retarded osmosis membrane mass exchanger, Journal of Membrane Science, 445 (2013) 211-219.
[20] C. Klaysom, T. Cath, T. Depuydt, I.F.J. Vankelecom, Forward and pressure retarded osmosis: potential solutions for global challenges in energy and water supply, Chemical Society Reviews, 42 (2013) 6959-6989.
[21] L.D. Banchik, M.H. Sharqawy, J.H. Lienhard V, Effectiveness-mass transfer units (ε-MTU) model of a reverse osmosis membrane mass exchanger, Journal of Membrane Science, 458 (2014) 189-198.
[22] W.M. Kays, A.L. London, Compact Heat Exchangers, 3rd ed., McGraw-Hill, New York, 1984.
[23] J.H. Lienhard IV, J.H. Lienhard V, A Heat Transfer Textbook, 3rd ed., Phlogiston Press, Cambridge, MA, 2008.
[24] S. Klein, Engineering Equation Solver V9.438, 2013.
[25] J.R. McCutcheon, M. Elimelech, Modeling water flux in forward osmosis: implications for improved membrane design. American Institute of Chemical Engineers Journal, 53-7 (2007) 1736–1744.
[26] M. Wilf, The Guidebook to Membrane Desalination Technology, Balaban Desalination Publications, Hopkinton, MA (2007).
[27] G.D. Mehta, S. Loeb, Internal polarization in the porous substructure of a semipermeable membrane under pressure-retarded osmosis, Journal of Membrane Science 4 (1978), 261–265.

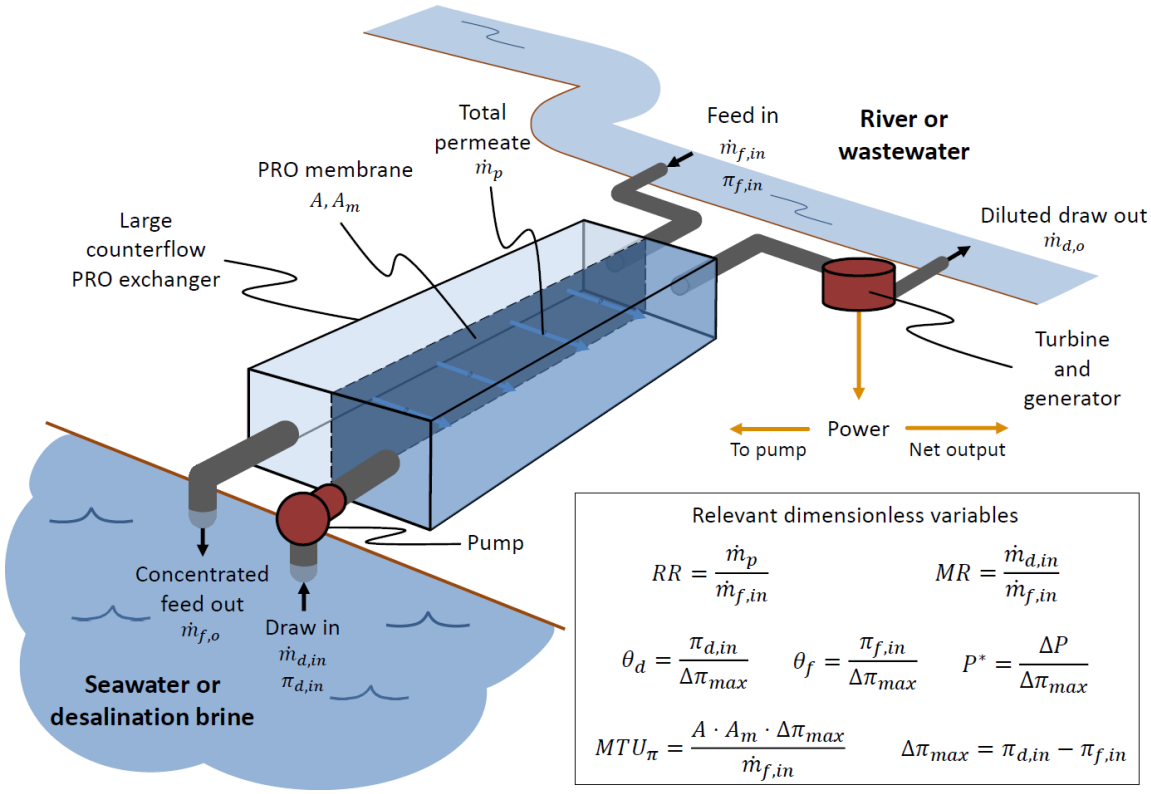

Fig. 1 Schematic diagram of a simplified PRO system with relevant dimensionless parameters. The total permeate is depressurized through the hydro-turbine to produce useful power.

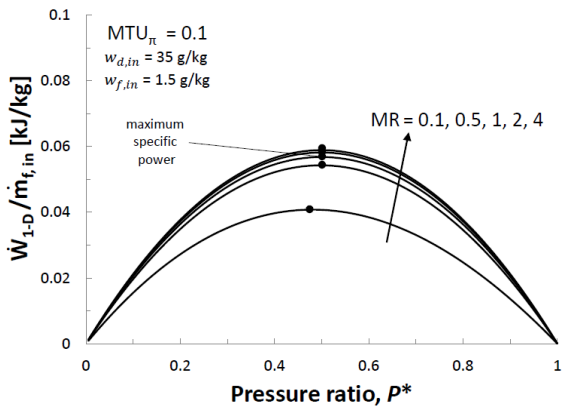

(a)

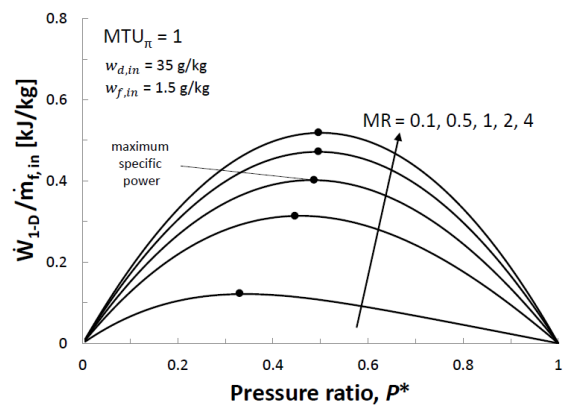

(b)

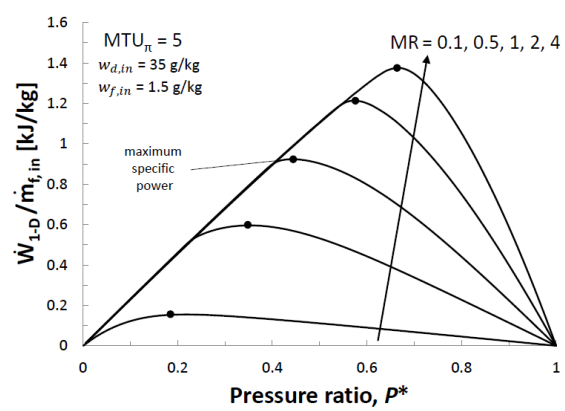

(c)

Fig. 2 Specific power vs. pressure ratio for various mass flow rate ratios in a one-dimensional, counterflow PRO membrane with seawater and river water as working fluids: (a) MTU$_\pi$ = 0.1 (b) MTU$_\pi$ = 1 (c) MTU$_\pi$ = 5

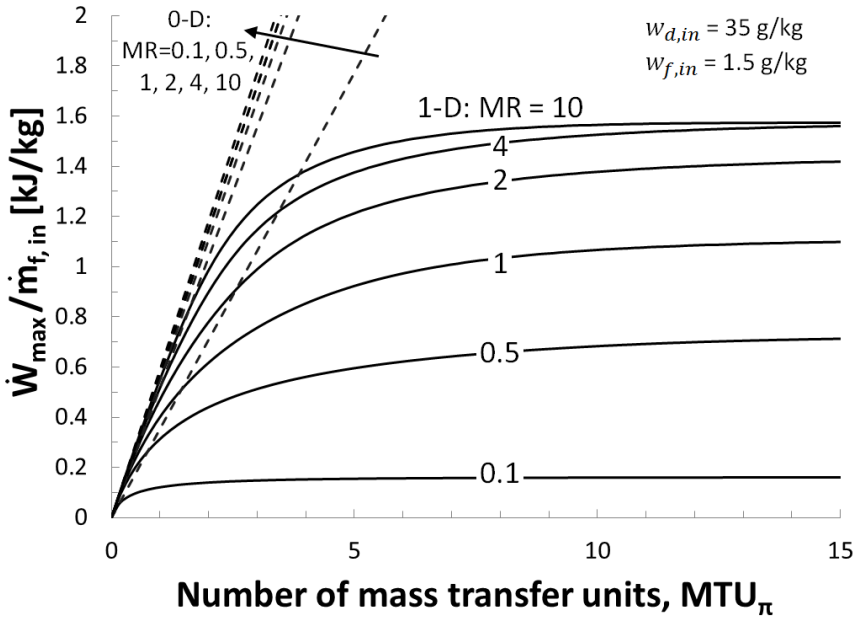

Fig. 3 Specific maximum power vs. MTU_{π} for various mass flow rate ratios in a one-dimensional (solid line), counterflow PRO membrane with seawater and river water as working fluids. The specific maximum power for a zero-dimensional (dashed line) membrane is linearly proportional to MTU_{π}.

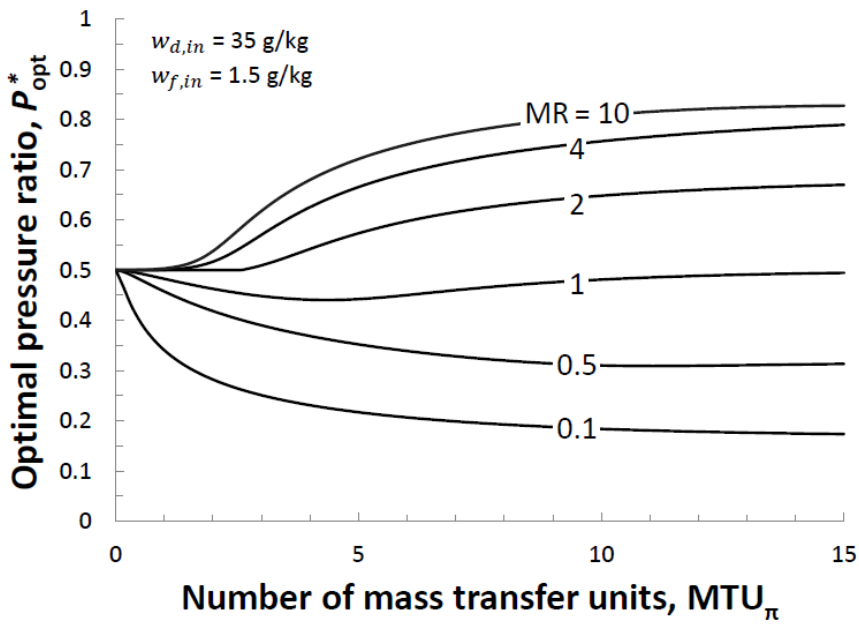

Fig. 4 Optimal pressure ratio vs. MTU_π for various mass flow rate ratios in a one-dimensional, counterflow PRO membrane with seawater and river water as working fluids.

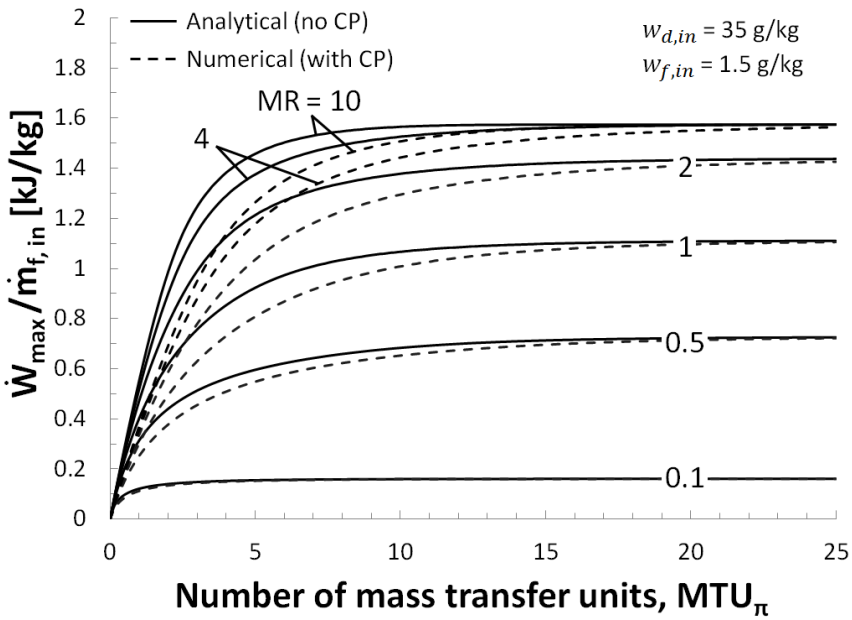

Fig. 5 Specific maximum power vs. MTU_{π} for various mass flow rate ratios in a one-dimensional, counterflow PRO membrane with seawater and river water as working fluids. Numerical results which incorporate concentration polarization are denoted by the dashed lines.

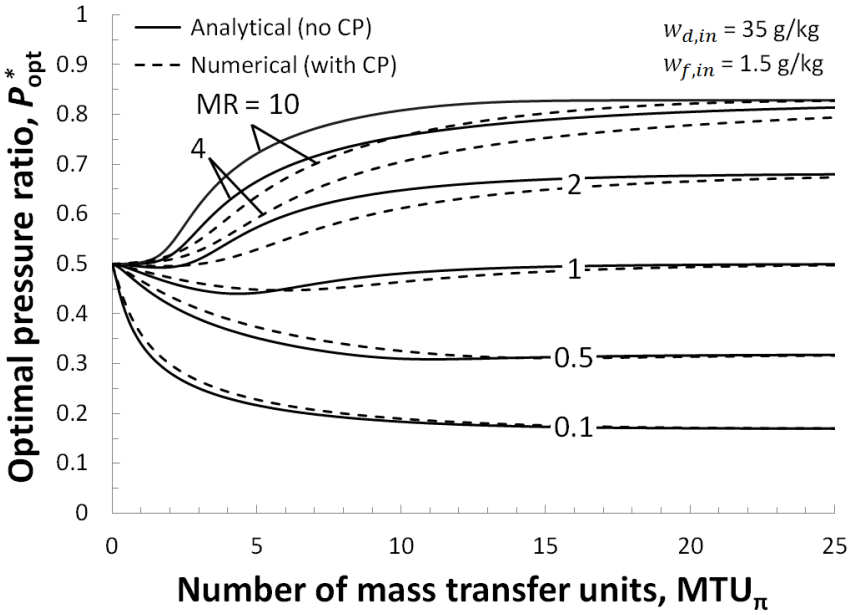

Fig. 6 Optimal pressure ratio vs. MTU_π for various mass flow rate ratios in a one-dimensional, counterflow PRO membrane with seawater and river water as working fluids. Numerical results which incorporate concentration polarization are denoted by the dashed lines.

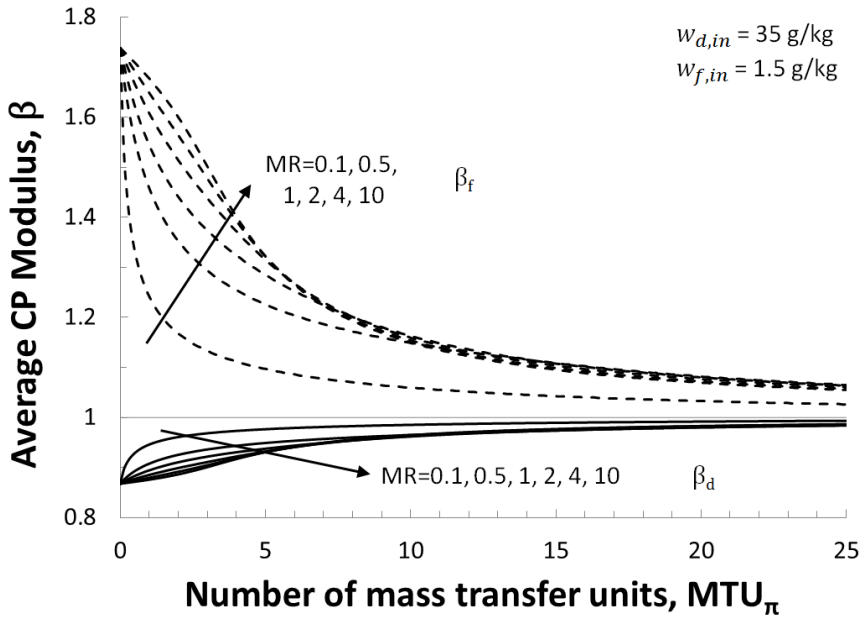

Fig. 7 Average concentration polarization moduli vs. MTU_{π} for various mass flow rate ratios in a one-dimensional, counterflow PRO membrane with seawater and river water as working fluids. Solid lines denote the draw-side external CP modulus and dashed lines denote the feed-side internal CP modulus.

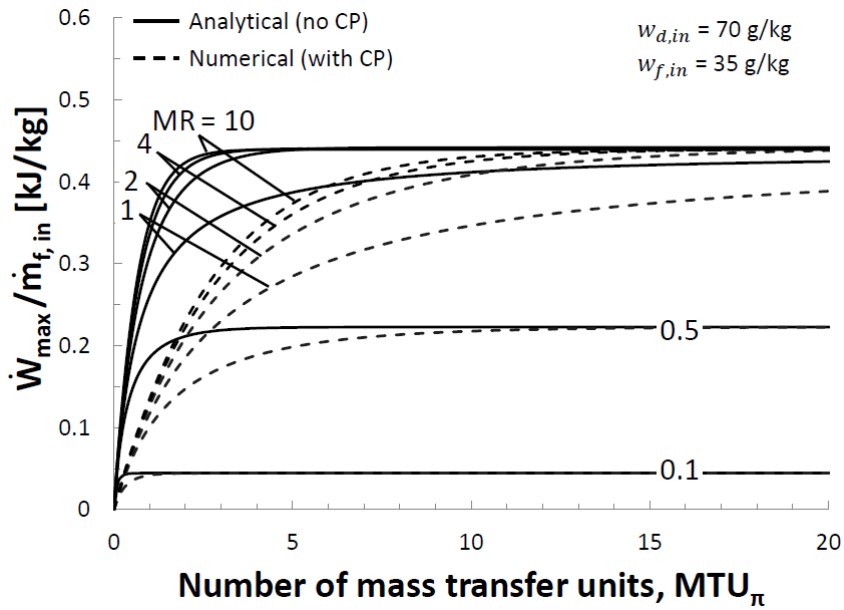

(a)

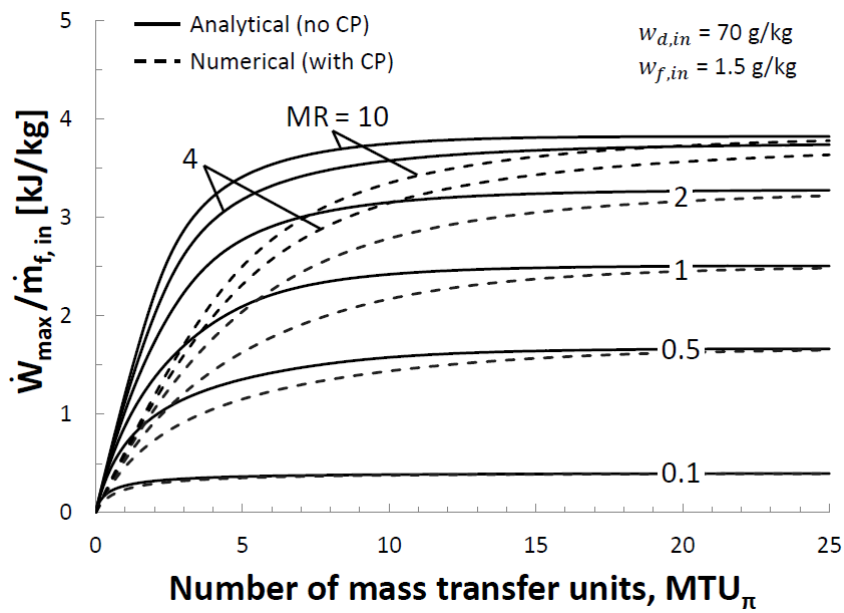

(b)

Fig. 8 Specific maximum power vs. MTU_{π} for various mass flow rate ratios in a one-dimensional, counterflow PRO membrane with: (a) brine and seawater and (b) brine and wastewater or river water as working fluids. Numerical results which include concentration polarization are denoted by the dashed lines.

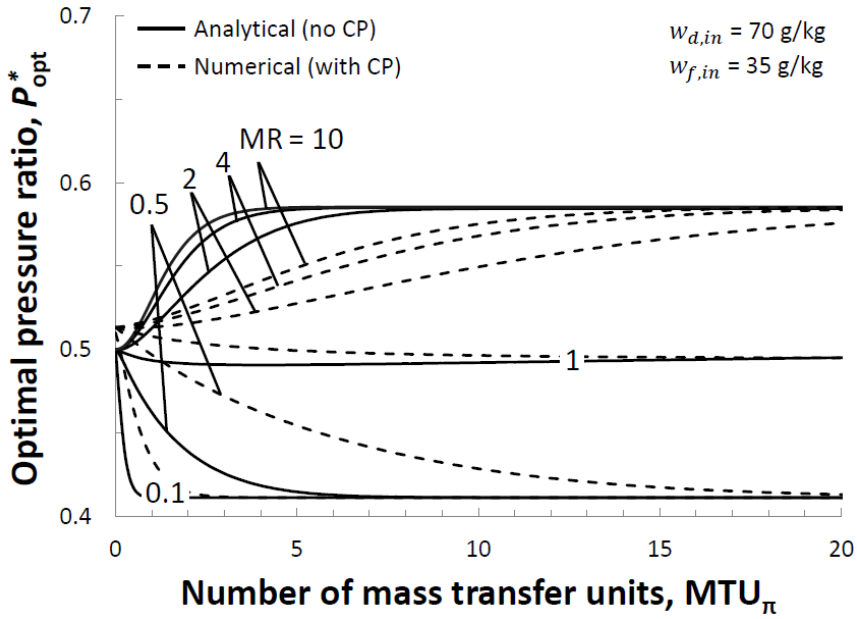

(a)

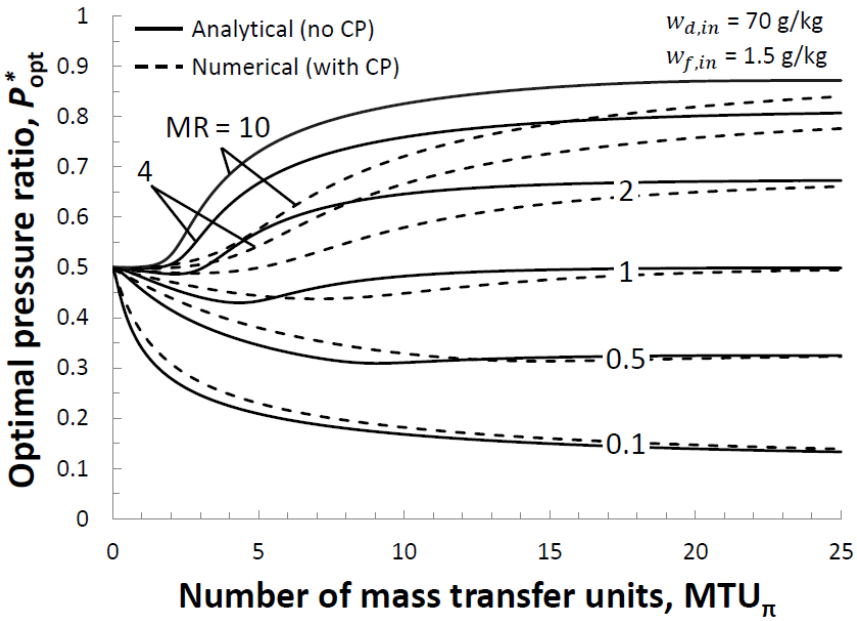

(b)

Fig. 9 Optimal pressure ratio vs. MTU_π for various mass flow rate ratios in a one-dimensional, counterflow PRO membrane with: (a) brine and seawater and (b) brine and wastewater or river water as working fluids. Numerical results which include concentration polarization are denoted by the dashed lines.

Table 1. Overall maximum power results

Draw and feed	Modified van 't Hoff coefficient, *C* [kPa-kg/g]	Overall maximum power [kJ/kg feed]	Optimal pressure ratio, P^*
Seawater and river water (35 and 1.5 g/kg)	73.07	1.57	0.83
Brine and seawater (70 and 35 g/kg)	76.76	0.44	0.59
Brine and wastewater (70 and 1.5 g/kg)	78.42	3.82	0.87

Table 2. Numerical model inputs

Input	Values/Range
Ambient temperature, T_0	25 °C
Modified water permeability coefficient, A [26]	3.07×10^{-6} kg/m^2 s kPa
Draw side mass transfer coefficient, k_d [25]	1.75×10^{-5} m/s
Solute resistance to diffusion (PRO), K [25]	2.24×10^{5} s/m
Feed mass flow rate, $\dot{m}_{f,in}$	1 kg/s
Inlet draw salinity, $w_{d,in}$	70 g/kg and 35 g/kg
Inlet feed salinity, $w_{f,in}$	35 g/kg and 1.5 g/kg
Mass flow rate ratio, MR	0.1, 0.5, 1, 2, 4, 10
Trans-membrane pressure difference, ΔP	0 – 4219.7 kPa
Membrane area, A_m	0 – 2003 m^2